

REPORT DOCUMENTATION PAGE			Form Approved OMB NO. 0704-0188		
<p>The public reporting burden for this collection of information is estimated to average 1 hour per response, including the time for reviewing instructions, searching existing data sources, gathering and maintaining the data needed, and completing and reviewing the collection of information. Send comments regarding this burden estimate or any other aspect of this collection of information, including suggestions for reducing this burden, to Washington Headquarters Services, Directorate for Information Operations and Reports, 1215 Jefferson Davis Highway, Suite 1204, Arlington VA, 22202-4302. Respondents should be aware that notwithstanding any other provision of law, no person shall be subject to any penalty for failing to comply with a collection of information if it does not display a currently valid OMB control number.</p> <p>PLEASE DO NOT RETURN YOUR FORM TO THE ABOVE ADDRESS.</p>					
1. REPORT DATE (DD-MM-YYYY)		2. REPORT TYPE New Reprint		3. DATES COVERED (From - To) -	
4. TITLE AND SUBTITLE Enhanced Stability of PtRu Supported on N-Doped Carbon for the Anode of a DMFC			5a. CONTRACT NUMBER W911NF-09-1-0528		
			5b. GRANT NUMBER		
			5c. PROGRAM ELEMENT NUMBER 611103		
6. AUTHORS P. Joghee, S. Pylypenko, T. Olson, A. Dameron, A. Corpuz, H. N. Dinh, K. Wood, K. O'Neill, K. Hurst, G. Bender, T. Gennett, B. Pivovar, R. O'Hayre			5d. PROJECT NUMBER		
			5e. TASK NUMBER		
			5f. WORK UNIT NUMBER		
7. PERFORMING ORGANIZATION NAMES AND ADDRESSES Colorado School of Mines Research Administration 1500 Illinois St Golden, CO 80401 -1911			8. PERFORMING ORGANIZATION REPORT NUMBER		
9. SPONSORING/MONITORING AGENCY NAME(S) AND ADDRESS(ES) U.S. Army Research Office P.O. Box 12211 Research Triangle Park, NC 27709-2211			10. SPONSOR/MONITOR'S ACRONYM(S) ARO		
			11. SPONSOR/MONITOR'S REPORT NUMBER(S) 54646-CH-PCS.23		
12. DISTRIBUTION AVAILABILITY STATEMENT Approved for public release; distribution is unlimited.					
13. SUPPLEMENTARY NOTES The views, opinions and/or findings contained in this report are those of the author(s) and should not be construed as an official Department of the Army position, policy or decision, unless so designated by other documentation.					
14. ABSTRACT The performance and long-term stability of a direct-methanol fuel cell (DMFC) employing PtRu supported on nitrogen-modified carbon is compared with that of PtRu/C (Hi-spec 5000). The long-term stability test is carried by means of accelerated degradation testing (ADT) at an anodic potential of 0.8 V vs. DHE for 640h. The initial DMFC performance of the MEA					
15. SUBJECT TERMS direct methanol fuel cell, accelerated degradation testing, durability, nitrogen doping, catalysis					
16. SECURITY CLASSIFICATION OF:		17. LIMITATION OF ABSTRACT		15. NUMBER OF PAGES	19a. NAME OF RESPONSIBLE PERSON
a. REPORT UU	b. ABSTRACT UU	c. THIS PAGE UU	UU		19b. TELEPHONE NUMBER 303-273-3952

## Report Title

Enhanced Stability of PtRu Supported on N-Doped Carbon for the Anode of a DMFC

### ABSTRACT

The performance and long-term stability of a direct-methanol fuel cell (DMFC) employing PtRu supported on nitrogen-modified carbon is compared with that of PtRu/C (Hi-spec 5000). The long-term stability test is carried by means of accelerated degradation testing (ADT) at an anodic potential of 0.8 V vs. DHE for 640h. The initial DMFC performance of the MEA containing PtRu/C (N-doped) is slightly lower than that of the PtRu/C (Hi-SPEC) because of the lower ECSA of the former. After 640h ADT, the anode ECSA loss is found to be 21% and 26% for the PtRu/C (N-doped) and PtRu/C (Hi-SPEC), respectively. Electrochemical analyzes reveal that cathode of the MEA with PtRu/C (N-doped) is less contaminated with Ru. It is further corroborated by post-mortem analysis done by scanning electron microscopy (SEM) associated with EDS, which indicates 4.8 and 8.2 at.% Ru accumulation, respectively, in the cathodes of the PtRu/C (N-doped) and PtRu/C (Hi-SPEC) MEAs after 640h ADT. Although both MEAs sustain anode and cathode ECSA losses, the performance for the PtRu/C (N-doped) MEA is improved by 28% and 8% after initial and long-term ADT, while

---

**REPORT DOCUMENTATION PAGE (SF298)**  
**(Continuation Sheet)**

---

Continuation for Block 13

ARO Report Number 54646.23-CH-PCS  
Enhanced Stability of PtRu Supported on N-Dop ...

Block 13: Supplementary Note

© 2012 . Published in Journal of the Electrochemical Society, Vol. Ed. 0 159, (11) (2012), ( (11). DoD Components reserve a royalty-free, nonexclusive and irrevocable right to reproduce, publish, or otherwise use the work for Federal purposes, and to authorize others to do so (DODGARS §32.36). The views, opinions and/or findings contained in this report are those of the author(s) and should not be construed as an official Department of the Army position, policy or decision, unless so designated by other documentation.

Approved for public release; distribution is unlimited.



the society for solid-state  
and electrochemical  
science and technology

Journal of The Electrochemical Society

## Enhanced Stability of PtRu Supported on N-Doped Carbon for the Anode of a DMFC

Prabhuram Joghee, Svitlana Pylypenko, Tim Olson, Arrelaine Dameron, April Corpuz, Huyen N. Dinh, Kevin Wood, Kevin O'Neill, Katherine Hurst, Guido Bender, Thomas Gennett, Bryan Pivovar and Ryan O'Hayre

*J. Electrochem. Soc.* 2012, Volume 159, Issue 11, Pages F768-F778.  
doi: 10.1149/2.063211jes

---

**Email alerting  
service**

Receive free email alerts when new articles cite this article - sign up in the box at the top right corner of the article or [click here](#)

---

---

To subscribe to *Journal of The Electrochemical Society* go to:  
<http://jes.ecsdl.org/subscriptions>

---



## Enhanced Stability of PtRu Supported on N-Doped Carbon for the Anode of a DMFC

Prabhuram Joghee,<sup>a,\*</sup> Svitlana Pylypenko,<sup>a,b,\*</sup> Tim Olson,<sup>b</sup> Arrelaine Dameron,<sup>b</sup> April Corpuz,<sup>c</sup> Huyen N. Dinh,<sup>b,\*</sup> Kevin Wood,<sup>a,\*\*</sup> Kevin O'Neill,<sup>b</sup> Katherine Hurst,<sup>b</sup> Guido Bender,<sup>b,\*</sup> Thomas Gennett,<sup>b</sup> Bryan Pivovar,<sup>b,\*</sup> and Ryan O'Hayre<sup>a,z</sup>

<sup>a</sup>Department of Metallurgical & Materials Engineering, Colorado School of Mines, Golden, Colorado 80401, USA

<sup>b</sup>National Renewable Energy Laboratory, Golden, Colorado 80401, USA

<sup>c</sup>Department of Chemistry, Colorado School of Mines, Golden, Colorado 80401, USA

The performance and long-term stability of a direct-methanol fuel cell (DMFC) employing PtRu supported on nitrogen-modified carbon is compared with that of PtRu/C (Hi-spec 5000). The long-term stability test is carried by means of accelerated degradation testing (ADT) at an anodic potential of 0.8 V vs. DHE for 640h. The initial DMFC performance of the MEA containing PtRu/C (N-doped) is slightly lower than that of the PtRu/C (Hi-SPEC) because of the lower ECSA of the former. After 640h ADT, the anode ECSA loss is found to be ~21% and ~26% for the PtRu/C (N-doped) and PtRu/C (Hi-SPEC), respectively. Electrochemical analyzes reveal that cathode of the MEA with PtRu/C (N-doped) is less contaminated with Ru. It is further corroborated by post-mortem analysis done by scanning electron microscopy (SEM) associated with EDS, which indicates 4.8 and 8.2 at.% Ru accumulation, respectively, in the cathodes of the PtRu/C (N-doped) and PtRu/C (Hi-SPEC) MEAs after 640h ADT. Although both MEAs sustain anode and cathode ECSA losses, the performance for the PtRu/C (N-doped) MEA is improved by ~28% and ~8% after initial and long-term ADT, while the performance for the PtRu/C (Hi-SPEC) MEA is improved by ~20% after initial and decreased by ~3% after long-term ADT.

© 2012 The Electrochemical Society. [DOI: 10.1149/2.063211jes] All rights reserved.

Manuscript submitted July 10, 2012; revised manuscript received August 20, 2012. Published September 18, 2012.

Direct methanol fuel cells (DMFCs) are considered as potential portable power sources for electronic devices owing to the high energy density of methanol, their benign operating conditions and their relative compactness.<sup>1-3</sup> For commercial implementation of a DMFC, improving lifetime reliability and stability are key factors. Improving the lifetime stability of the membrane electrode assembly (MEA) in a DMFC remains a challenging issue due to the degradation of components under the strong chemical and electrical potential gradients experienced in a fuel cell. In recent years, a substantial amount of research has been carried out to gain insight into DMFC MEA degradation.<sup>4-11</sup> It is broadly understood that the DMFC undergoes both recoverable and irrecoverable losses while operating under lifetime tests over a wide range of operating conditions. Voltage losses that occur due to water flooding at the cathode, surface oxidation of Pt in the cathode and CO<sub>2</sub> accumulation at the anode are recoverable.<sup>5,12</sup> However, losses that arise due to Ru dissolution from PtRu in the anode and crossover of Ru to cathode, electrode delamination, catalyst surface area loss due to dissolution and/or agglomeration, and changes in the hydrophilic/hydrophobic balance of the electrodes are irrecoverable.<sup>13-17</sup> In regards to Ru instabilities, Piela et al. have conducted a detailed study on the dissolution of Ru from state-of-the-art PtRu black catalysts and its subsequent migration and contamination of cathodes in a DMFC stack under pre-humidified conditions.<sup>13</sup> Ru contamination in the cathode typically leads to voltage losses in a DMFC on the order of ~40–60 mV by reducing the oxygen reduction reaction (ORR) and cathode's ability to handle methanol crossover.<sup>13,18</sup>

Because of these issues, several strategies have been adapted to enhance the stability of PtRu.<sup>19-21</sup> For instance, Chang et al.<sup>19</sup> reported that an annealed (>200°C) PtRu containing RuO<sub>x</sub>H<sub>y</sub> species exhibited a relatively higher stability during voltammetric investigations compared with non-annealed samples. In a similar fashion, PtRu catalysts formed by decorating Pt metal with ruthenium oxide nanosheets (HRONs) have shown greater stability when compared against conventional PtRu catalysts in accelerated stability tests conducted in the potentiostatic mode.<sup>20,21</sup> In another approach, it has been demonstrated that incorporation of Au into PtRu stabilizes the PtRu catalyst against the dissolution of Ru.<sup>22</sup> It has been hypothesized that Au incorporation in PtRu may lead to charge transfer from Ru to Au, thereby

increasing the oxidation state of Ru to Ru<sup>3+</sup> in the Au/PtRu catalyst. The resulting Ru<sup>3+</sup> is stabilized because it requires a higher anodic potential to undergo dissolution during DMFC operation.

In an increasingly well-studied alternative approach, researchers have used novel catalyst support materials,<sup>23-25</sup> including chemically functionalized or modified carbon support materials that can provide better anchoring sites to stabilize the supported Pt or PtRu nanoparticles.<sup>26-37</sup> Among these later approaches, functionalization of high surface area carbon supports with nitrogen has gained particular momentum and has been demonstrated to yield several beneficial effects, including improving the dispersion and reducing the size of the Pt particles nucleated on the support,<sup>38,39</sup> increasing the interaction (and hence stability) of the Pt nanoparticles with the support, and increasing the electrical conductivity and hydrophilicity of the support itself.<sup>40-42</sup> These effects are in-part attributed to the fact that nitrogen-functionalization of the carbon support can alter the pi bonding and increase the basicity, which in-turn enhances the Pt-C bond strength, resulting in stabilization of the Pt particles.<sup>43-45</sup> PtRu nanoparticles supported on nitrogen-doped carbon black<sup>27</sup> and carbon nanotubes (CNTs)<sup>26,28</sup> have shown higher electrochemically active surface area (ECSA) than their undoped counterparts, which results in higher intrinsic and mass activity toward the methanol oxidation reaction (MOR). Hsu et al.<sup>34</sup> have reported that Pt nanoparticle catalysts supported on nitrogen-doped CNTs show 15-fold higher MOR activities than a standard commercial Pt/C catalyst (E-TEK) after undergoing a potentiometric accelerated durability test for 2000 cycles. Interestingly, PtRu nanoparticles supported on a nitrogen-doped carbon nanotube-graphene hybrid nanostructure (NCNT-GHN) yielded nearly 30% higher power density and maintained higher voltage (nearly 100 mV) compared with PtRu nanoparticles supported on undoped CNTs when used in the anode of a DMFC during durability testing for 80h.<sup>33</sup>

Our group has recently conducted model-catalyst durability studies using Pt and PtRu nanoparticles electrodeposited as well as sputtered on nitrogen-doped highly oriented pyrolytic graphite (HOPG) to gain fundamental insight into the interactions between the nanoparticles and the functionalized carbon support.<sup>29,32,45</sup> The morphology and stability of Pt and PtRu was significantly improved during electrochemical durability cycling tests when the HOPG support was doped with relatively higher amounts of nitrogen (> 4%) as compared to undoped supports or supports doped with smaller levels of nitrogen.<sup>46</sup> It has been attributed that the lone pair of electrons on the sp<sup>2</sup> orbital at (pyridinic) nitrogen sites in the plane of carbon rings immobilizes

\*Electrochemical Society Active Member.

\*\*Electrochemical Society Student Member.

<sup>z</sup>E-mail: rohayre@mines.edu

the Pt and PtRu particles more firmly, which results in higher stability, and that multi-nitrogen functionalities are more effective than isolated substitutional nitrogen defects.<sup>33,46</sup>

In the present work, the above strategy has been followed to prepare nitrogen-doped high surface area Vulcan XC-72 carbon sputtered with PtRu in order to evaluate its performance and durability in the anode of a DMFC. The performance of this nitrogen-doped PtRu/C catalyst is compared against an MEA made from a state-of-the-art commercial PtRu/C (Hi-SPEC) catalyst. The PtRu composition (1:1 at.%) and the metal loading (30 wt%) on carbon are similar for both catalysts. The durability test has been performed by means of a potentiostatic accelerated degradation test (ADT) at 0.8 V (anode potential) vs. dynamic hydrogen electrode (DHE) for 640h. The ADT at 0.8 V vs. DHE has been applied instead of a normal operating cell voltage (usually 0.2 to 0.4 V) for the durability test because this high potential accelerates the dissolution of Ru,<sup>13,18,47</sup> which is used to examine and compare the stability aspects of the PtRu supported on N-doped carbon with the conventional PtRu/C catalyst. Additionally, during long-term DMFC operation short circuits, fuel starvation, or cell reversal may occur and during such episodes the anode can experience high potentials above 0.5 V.<sup>18,47</sup> Under such circumstances, the ADT at 0.8 V can provide additional information on the durability performance of the DMFC. Therefore, this work provides new insights into the stability of PtRu supported on nitrogen doped carbon, and compliments our recently reported work pertinent to long-term durability testing carried out under normal DMFC operating conditions.<sup>48</sup>

### Experimental

**Preparation of PtRu (N-doped-carbon) catalyst.**— PtRu(1:1) supported on nitrogen-doped carbon (PtRu/C (N-doped)) was prepared as an in-house catalyst. Initially, 500 mg of commercially available carbon powder (Cabot Vulcan XCR72R) was subjected to ion implantation with a non-mass separated nitrogen ion beam at room temperature for a period of 60 min with the ion beam energy of 100 eV and beam current of 13 mA. Subsequently, PtRu was incorporated onto the N-doped carbon powder by means of magnetron sputtering from a 50:50 PtRu alloy target. The sputtering was carried out by purging argon as the sputter gas with 10 mol% O<sub>2</sub> for a period of 60 min at 25 mTorr with DC power of 45 W. The details on the custom vacuum chamber used for the combined powder ion-implantation/sputtering process have been described elsewhere.<sup>49</sup>

**Physicochemical characterization of PtRu/C (N-doped) and PtRu/C (Hi-SPEC) catalysts.**— The initial composition of the PtRu/C (N-doped) was measured by X-ray fluorescence (XRF) using a maXXi 5/PIN XRF instrument (Roentgen Analytic) equipped with a tungsten target. The XRF composition was obtained by comparison with calibrated Pt<sub>1-x</sub>Ru<sub>x</sub> standards using software provided by the XRF manufacturer. Thermogravimetric analysis (TGA) was used to determine the total metal content of the PtRu/C (N-doped) catalyst powders. The TGA was done using the TA Q600 (TA Instruments, New Castle, DE) by feeding 100 mL min<sup>-1</sup> of synthetic air (80% N<sub>2</sub>, 20% O<sub>2</sub>) with a heating rate of 5°C min<sup>-1</sup> to a temperature of 850°C. It is assumed that the final mass at 850°C is composed of RuO<sub>2</sub> and Pt. The X-ray Photoelectron Spectroscopy (XPS) analysis of the PtRu/C (N-doped) was carried out using a Kratos Nova XPS with a monochromatic Al K-alpha source operated at 300 W. Data analyzes was performed using Casa XPS software and included subtraction of the linear background for O 1s and N 1s and the Shirley background for Pt 4f, Ru 3p and combined C 1s/Ru 3d regions.<sup>50</sup> Charge referencing was performed using the graphitic peak at 284.6 eV. The detailed information on the curve-fitting procedure is given elsewhere.<sup>46</sup>

**MEA fabrication using PtRu/C (N-doped) and PtRu/C (Hi-SPEC) and DMFC testing.**— MEAs with area 5 cm<sup>2</sup> were fabricated by the spray-coating method using the protocol described elsewhere.<sup>51</sup> Briefly, catalyst inks for the anode and the cathode were prepared by mixing appropriate amounts of 30 wt% PtRu/C (N-doped) or PtRu/C

(Hi-SPEC) and 40 wt% Pt/C (JM Hi-spec 4000), respectively, with isopropyl alcohol and ultrasonicated for 15 min. Then, 30 wt% of Nafion solution was added to the mixture and further ultrasonicated for 10 min. Subsequently, the prepared PtRu/C (N-doped) or PtRu/C (Hi-SPEC) and Pt/C homogeneous catalyst inks were sprayed on either side of pretreated Nafion 117 membranes. The catalyst loadings were maintained to 2 mg cm<sup>-2</sup> for both the anodes and cathodes of the MEAs. Finally, the MEAs were hot pressed at a temperature of 135°C under a load of 133 kg for 10 min. To test DMFC performance, the MEAs were assembled in single-cell test fixtures by placing micro porous carbon coated carbon paper contains 5 wt% PTFE (Sigracet, Model 25 BC), which acted as a gas diffusion layer (GDL) on either side of the MEAs. Serpentine-type graphite separators with channel dimension of 1 mm × 1 mm (depth × width) were employed. After assembling the MEAs, preconditioning was carried out by a two-step process involving hydrogen-air testing prior to methanol-air conditioning to establish a maximum performance of the cell.<sup>52</sup> Initially, the cell was preconditioned by discharging at 0.6 V for 2h by feeding humidified H<sub>2</sub> (105 mL min<sup>-1</sup>) and air (350 mL min<sup>-1</sup>) to the anode and cathode, respectively, at 80°C. Then, the cell voltage was maintained at 0.6 V for 10 min and 0.8 V for 5 min and this discharging cycle was repeated for 20h. In the subsequent step, the cell was discharged at a constant current of 0.1 A using 0.5 M methanol (2 mL min<sup>-1</sup>) and humidified air (200 mL min<sup>-1</sup>) at 80°C for 6h. After preconditioning, the DMFC performance curves were obtained by feeding 1 M methanol (2 mL min<sup>-1</sup>) and humidified air (200 mL min<sup>-1</sup>) to the anode and cathode, respectively, at ambient pressure and at 80°C. The DMFC performance testing was carried out galvanostatically by altering the current in 15 min steps and the corresponding voltage values were recorded with a commercial test station (Teledyne Energy Systems, Inc., USA). The voltage values recorded for the last 5 min at each current step were averaged and used for plotting the polarization curves.

**ADT for the MEAs.**— The ADT study for each cell was conducted for 640h using a potentiostat (Solartron Analytical, Model 1470E, USA) under an ADT protocol described in detail previously<sup>8</sup> with interruption every 80h to measure the ECSA of the electrodes, test DMFC performance, and acquire MOR polarization of the anode. Briefly, the ADT protocol involved feeding the anode (which served as the working electrode) with humidified N<sub>2</sub> (100 mL min<sup>-1</sup>), while the cathode (which acted as the counter and reference electrode) was fed with humidified H<sub>2</sub> (100 mL min<sup>-1</sup>). The anode potential was maintained at 0.8 V vs. DHE during the ADT at ambient pressure and at a temperature of 30°C. During the ADT study, testing was interrupted for every 80 h to conduct detailed electrochemical measurements including CO stripping voltammetry, cyclic voltammetry (CV) and linear sweep voltammetry (LSV) using a potentiostat (Solartron Analytical, Model 1470E, USA).

**Electrochemical characterization of MEAs.**— CO stripping voltammetry was used to determine changes to the ECSA of the anode and changes to the state of cathode over the course of the ADT. To perform CO stripping for the anode, high-purity humidified 0.1% CO in argon (200 mL min<sup>-1</sup>) and H<sub>2</sub> (100 mL min<sup>-1</sup>) were fed to anode and cathode, respectively. For the cathode CO stripping, the respective gases were switched, i.e. 0.1% CO in argon (200 mL min<sup>-1</sup>) and H<sub>2</sub> (100 mL min<sup>-1</sup>) were fed to the cathode and anode, respectively. For each stripping experiment, 0.1% CO in argon was fed to the electrode of interest (anode/cathode) while its potential was maintained at 0.1 V for 30 min. Then, humidified N<sub>2</sub> (200 mL min<sup>-1</sup>) was fed to the electrode for another 30 min while still maintaining the potential at 0.1 V. Subsequently, the CO stripping curves were collected in the potential region from 0.1 to 0.9 V at a scan rate of 5 mV sec<sup>-1</sup> at 25°C under a back pressure. The ECSA of the cathode was measured by CV before ADT and at periodic intervals during the ADT. The ECSA was calculated from the charges associated with the hydrogen adsorption and desorption peaks formed in the potential region from 0 to 0.4 V vs. DHE during the CV. The CV for the cathode was performed by

purging  $N_2$  ( $20 \text{ mL min}^{-1}$ ) and  $H_2$  ( $50 \text{ mL min}^{-1}$ ) to the anode and cathode, respectively, in the potential region from 0 to 1.0 V at a scan rate of  $20 \text{ mV sec}^{-1}$  at  $25^\circ\text{C}$  without any back pressure.

Activity of the anode was determined from the MOR polarization curves before ADT and at periodic intervals during the ADT. The MOR polarization curves were collected using LSV by feeding 1 M methanol ( $2 \text{ mL min}^{-1}$ ) and hydrogen ( $100 \text{ mL min}^{-1}$ ) to the anode and cathode, respectively, in the potential region from 0 to 0.7 V at a scan rate of  $5 \text{ mV sec}^{-1}$  at  $80^\circ\text{C}$ . The effect of Ru migration to cathode of the cells after the 640h ADT period was evaluated by measuring the MOR response to methanol crossover at the cathode.<sup>53</sup> The methanol crossover experiment was conducted by feeding 0.5 M methanol ( $2 \text{ mL min}^{-1}$ ) and dry nitrogen ( $100 \text{ mL min}^{-1}$ ) to the anode and the cathode, respectively. The cathode acted as the working electrode and the potential was swept from 0 to 0.6 V at the scan rate of  $0.1 \text{ mV sec}^{-1}$ . The methanol permeating to the cathode was oxidized and protons formed during the course of methanol oxidation migrated to anode which acted as the reference electrode (reducing the protons to hydrogen gas).

*Post-mortem analyzes of MEAs by SEM-EDS.*— Elemental compositions for both the anodes and cathodes of the MEAs subjected to ADT were evaluated using a JEOL JSM-7000F Field Emission Microscope (SEM) equipped with a Genesis Energy Dispersive X-Ray Spectrometer (EDS). The MEA samples were placed in the liquid  $N_2$  and then cut into small pieces for cross-sectional analysis.

## Results and Discussion

*Physicochemical characterization of catalysts.*— TGA, XRF and XPS analysis results for the PtRu/C (N-doped) and PtRu/C (Hi-SPEC) catalysts are given in Table I. It can be seen from the Table that both the PtRu/C (N-doped) and PtRu/C (Hi-SPEC) catalysts have approximately 30 wt% of 1:1 PtRu on carbon. XPS analysis shows that the PtRu/C (N-doped) mainly consists of a mixture of anhydrous and hydrous Ru oxides. On the other hand, the PtRu/C (Hi-SPEC) has a significant amount of metallic Ru and Ru oxide species. From Table I, it can be seen that for the PtRu/C (Hi-SPEC) only a small amount of nitrogen is present and it shows a fairly narrow N1s spectrum (Figure 1a), indicating that nitrogen functionalities are most likely limited to pyrrolic, N-C=O and amine groups. In the case of PtRu/C (N-doped), the ion implantation introduces multiple nitrogen functionalities, which is evident from the appearance of a wide N1s spectrum

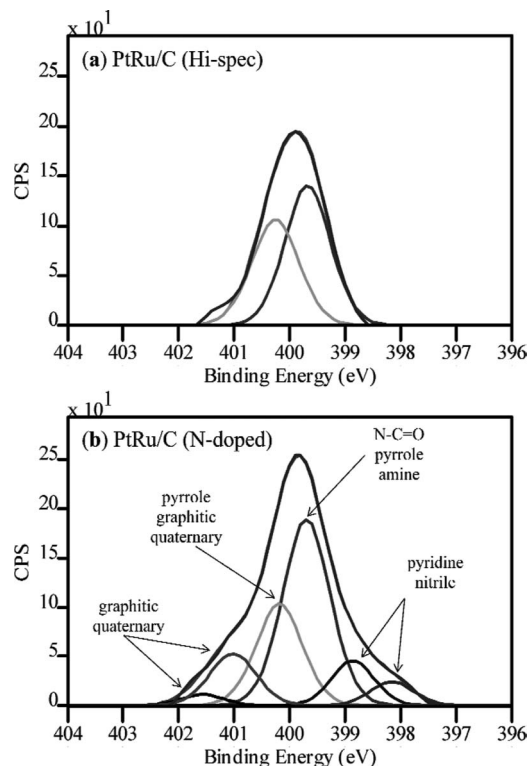


**Figure 1.** XPS high-resolution N1s spectra acquired from (a) PtRu/C (Hi-SPEC) and (b) PtRu/C (N-doped).

(Fig. 1b), suggesting the presence of graphitic, quaternary, pyridinic, C-N=O, pyrrolic, amine and nitrile groups.<sup>32,46</sup>

*Initial DMFC performance and electrochemical behavior of MEAs.*— Figure 2 compares the initial DMFC performance (2a), anode MOR polarization (2b), and anode CO stripping voltammetry curves (2c) for MEAs made with PtRu/C (N-doped) and PtRu/C (Hi-SPEC). The MEAs with PtRu/C (Hi-SPEC) and PtRu/C (N-doped) generated 180 and 160  $\text{mA cm}^{-2}$ , respectively, at 0.4 V. The lower performance of the MEA with PtRu/C (N-doped) is contrary to our recent report, in which a PtRu/C (N-doped) catalyst showed relatively higher initial performance than PtRu/C (Hi-SPEC).<sup>48</sup> As will be discussed in more detail later, this difference can likely be attributed to the significantly lower ECSA obtained for the PtRu/C (N-doped) catalyst used in this study. The performance trend is also reflected in the MOR activity comparison for the MEAs with PtRu/C (Hi-SPEC) and PtRu/C (N-doped) as shown in Fig. 2b. The onset potential of the MOR for PtRu/C (Hi-SPEC) is shifted negatively by  $\sim 40 \text{ mV}$  compared to that of the PtRu/C (N-doped) and the two anodes exhibit current densities of 300 and 260  $\text{mA cm}^{-2}$ , respectively, at 0.4 V vs DHE. The CO stripping voltammetry curves for the MEAs with PtRu/C (Hi-SPEC) and PtRu/C (N-doped) are shown in Fig. 2c. These voltammograms yield ECSA values of 126.6 and 56.1  $\text{m}^2 \text{ g}^{-1}$ , for the PtRu/C (Hi-SPEC) and PtRu/C (N-doped) anodes, respectively. The ECSA of PtRu/C (N-doped) is nearly 56% lower than that of the PtRu/C (Hi-SPEC), but the cell performance of the former is merely 11% lower than the latter. It is important to note that the 40 wt% Pt/C used in the cathode of two MEAs have nearly identical ECSA values (84.1 and 87.5  $\text{m}^2 \text{ g}^{-1}$  for the PtRu/C (Hi-SPEC) and PtRu/C (N-doped), respectively); and so it is believed that the initial differences in cell performance can be attributed to the differences in the anode catalysts. Interestingly, the MEA with PtRu/C (N-doped) shows reasonable cell performance despite having significantly lower ECSA. We hypothesize that if the PtRu/C (N-doped) could be prepared with the same ECSA as that of PtRu/C (Hi-SPEC) it might be possible to attain significantly greater

**Table I.** Elemental compositions of PtRu/C (N-doped) and PtRu/C (Hi-SPEC) catalysts.

Catalyst	PtRu/C (N-doped)	PtRu/C (Hi-SPEC)
Platinum, wt% <sup>a</sup>	19.8	18–21 <sup>b</sup>
Ruthenium, wt% <sup>a</sup>	10.2	9–11 <sup>b</sup>
Platinum, at.% (of total metal) <sup>a</sup>	52.6	50
Ruthenium, at.% (of total metal) <sup>a</sup>	47.3	50
	XPS data	
C 1s	87.8	89.2
O 1s	9.0	7.8
Pt 4f	1.0	1.2
Ru 3p	1.0	1.3
N 1s	1.2	0.6
Ru1,%Ru metallic	0.0	10.7
Ru2,%RuO <sub>2</sub> screened final state	3.8	32.1
Ru2,%RuO <sub>2</sub> .nH <sub>2</sub> O (or RuO <sub>x</sub> H <sub>y</sub> )	51.8	38.7
Ru3,%RuO <sub>2</sub> unscreened final state and /or RuO <sub>3</sub>	44.4	18.16

<sup>a</sup>Total metal weight percent of PtRu on carbon is measured by TGA and Pt:Ru ratio is determined by XRF.

<sup>b</sup>Data as provided by the manufacturer, Johnson Matthey on their website.

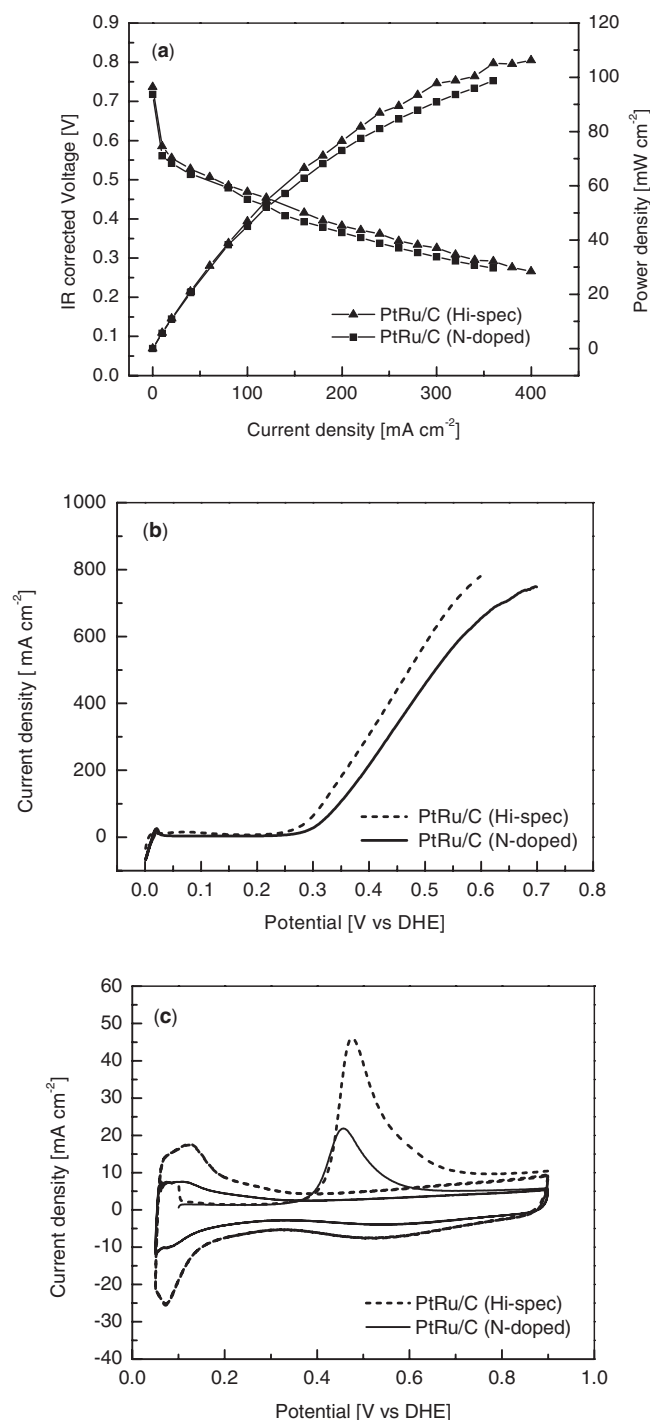


**Figure 2.** Comparison of (a) initial DMFC performance (80°C); (b) MOR activity for the anode (80°C) and (c) CO stripping voltammograms for the MEAs containing PtRu/C (Hi-SPEC) and PtRu/C (N-doped) (25°C).

performance enhancement. Although the exact reason for the lower ECSA of the PtRu/C (N-doped) catalyst is not clearly understood, it is speculated that variations/inhomogeneities and possible morphological modification of carbon associated with the nitrogen implantation and PtRu sputtering process, especially when fabricating the large batch of catalyst material (~3 g) needed for this study, may have contributed to the lower obtained ECSA. Because sputter-deposition of PtRu on high surface area carbon materials suffers from shadowing effects and does not take advantage of the preferential nucleation sites created during N-ion implantation,<sup>48</sup> it may be difficult for this

approach to attain the ECSA values that can be achieved from wet chemical deposition approaches, where shadowing effects are mitigated and preferential nucleation-site effects can play a significant role.<sup>38,54,55</sup>

Although the initial performance of the DMFC using PtRu/C (N-doped) is found to be slightly lower than that of the PtRu/C (Hi-SPEC), previous studies suggest that the presence of nitrogen in carbon support of the former should provide higher electrochemical stability and improved long-term cell performance under normal DMFC operating conditions.<sup>32,46,48</sup> However, in order to more aggressively probe PtRu stabilization effects in the N-doped carbon catalyst material, the PtRu/C (N-doped) and PtRu/C (Hi-SPEC) MEAs in this study were subjected to a high anodic potential ADT protocol, which expedites Ru dissolution. The ADT study involved running both MEAs at a potential of 0.8 V vs. DHE for 640h under the potentiostatic mode with a periodic interruption every 80h to evaluate the electrochemical degradation of the electrodes and to check DMFC performance.

*Effect of ADT on the electrochemical behaviors of MEAs.*— The anode CO stripping voltammograms for the PtRu/C (Hi-SPEC) and PtRu/C (N-doped) MEAs as function of ADT time are shown in Figure 3a-3b, while relative %ECSA loss vs. ADT time data extracted from these voltammograms are provided in Figure 3c. For the PtRu/C (Hi-SPEC) anode (Fig. 3a), initially a single narrow peak associated with the CO oxidation is observed with a peak potential at 0.47 V. After 200h ADT, the CO oxidation peak has shifted positively by ~20 mV with a peak potential at 0.49 V. For the PtRu/C (N-doped) anode (Fig. 3b), the CO oxidation peak is initially located at ~0.44 V and after 200h ADT it has shifted positively by only ~10 mV. In addition, the PtRu/C (N-doped) anode peak height and width shows less reduction during the ADT protocol. These results indicate a smaller loss of ECSA for the PtRu/C (N-doped) anode compared with the PtRu/C (Hi-SPEC) over the course of the ADT study. This point is further quantified by the relative ECSA loss curves depicted in Fig. 3c. This outcome suggests that less RuO<sub>x</sub>H<sub>y</sub> dissolution<sup>19,56</sup> may occur in the PtRu/C (N-doped) anode (which mainly consists of RuO<sub>x</sub>H<sub>y</sub> species as shown in Table I), during the initial stages of the ADT. This conclusion is further bolstered by the CO stripping results for the cathode, which will be discussed in the forthcoming section (see Fig. 4a). We hypothesize that the higher initial amounts of metallic Ru phase in the PtRu/C (Hi-SPEC) as shown in Table I preferentially dissolve during the initial stages of the ADT, thereby leading to the more rapid initial ECSA losses observed for this catalyst. After 400 and 640h ADT, even though there is a further decrease in the charging current of the CO oxidation peak (due to dissolution of Ru/RuO<sub>2</sub><sup>13,57</sup> and RuO<sub>x</sub>H<sub>y</sub><sup>19,56</sup> for the anodes of PtRu/C (Hi-SPEC) and PtRu/C (N-doped), respectively), there are no further shifts in the CO oxidation peak onset potential. This is most likely due to the electrochemical formation and conversion of mainly RuO<sub>2</sub> to higher oxide species during ADT at 0.8 V, which helps to mediate CO oxidation at an early potential.<sup>8,58,59</sup> It is understood that higher Ru-oxide species are simultaneously formed/converted and stabilized along with dissolution of Ru at 0.8 V vs. DHE, which will be discussed in more detail in the latter section. Because of the formation of these higher Ru-oxides, further ECSA loss in both catalysts is mostly mitigated at the longer 400 and 640h ADT intervals. The absolute values of the ECSA for both the catalysts after different intervals of ADT are given in Table II. After completion of the full 640h ADT study, the loss in ECSA for the PtRu/C (N-doped) and PtRu/C (Hi-SPEC) anodes is found to be ~21 and ~26%, respectively. In this study, even though we emphasize the ECSA loss is driven mainly by Ru dissolution in the context of observing a significant reduction of Ru dissolution for the MEA containing PtRu/C (N-doped) as compared with that of PtRu/C (Hi-SPEC), additional ECSA loss by particle agglomeration processes, especially on the anode of the MEAs subjected to ADT at 0.8 V vs. DHE for different periods of time is not ruled out,<sup>8</sup> although it would require a detailed investigation to fully separate these effects. Notably, however, one of our recent studies has shown that nitrogen

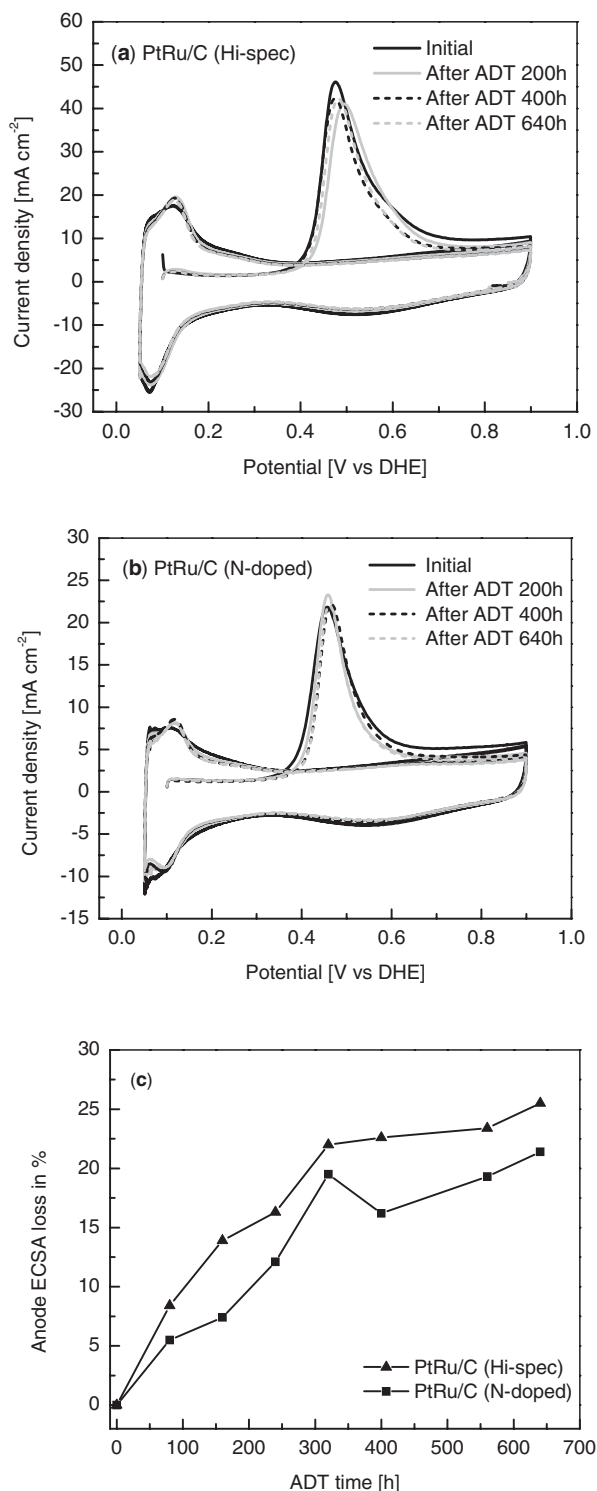


**Figure 3.** CO stripping voltammograms for the MEAs as a function of ADT time; (a) PtRu/C (Hi-SPEC), (b) PtRu/C (N-doped), and (c) Relative anode ECSA loss vs. ADT time extracted from the CO stripping voltammograms.

doping in the carbon substrate has the ability to control even the agglomeration of catalytic particles, thereby minimizing the ECSA loss by this mechanism as well.<sup>60</sup>

Figure 4 shows the CO stripping voltammograms for the cathodes (40 wt% Pt/C) of both MEAs as a function of ADT time. The initial CO stripping for both cathodes, obtained immediately after measuring initial DMFC performance, is shown in Fig. 4a. For the cathode of the MEA with PtRu/C (Hi-SPEC), a small CO oxidation peak at 0.55 V is apparent in addition to the primary CO oxidation peak associated with Pt at  $\sim 0.72$  V.<sup>61</sup> The observed peak at 0.55 V suggests the presence of trace amount of Ru species already on cathode of the MEA during this initial examination.<sup>62</sup> For the cathode of the MEA with PtRu/C (N-doped), the initial CO oxidation peak associated with Ru is not so prominent, and instead a larger CO oxidation peak for Pt is observed at  $\sim 0.75$  V. These results corroborate our hypothesis that dissolution and migration of Ru to the cathode is more severe during the initial conditioning and performance measurement period for the MEA containing PtRu/C (Hi-SPEC) as compared to the MEA containing PtRu/C (N-doped). As previously discussed, the presence of higher initial amounts of metallic Ru phase in the PtRu/C (Hi-SPEC) as shown in Table I may have led to greater preferential Ru dissolution and migration to the cathode during the initial DMFC break-in and performance testing period. The CO stripping voltammograms for the cathodes after ADT 200, 400 and 640h are shown in Figure 4b-4d. The first CO oxidation peak associated with Ru at 0.55 V gradually grows while the second CO oxidation peak at 0.74 V associated with Pt slowly diminishes for both MEAs, indicating an increasing amount of cathode Ru contamination coming from Ru/RuO<sub>2</sub> and RuO<sub>x</sub>H<sub>y</sub>, respectively, for the PtRu/C (Hi-SPEC) and PtRu/C (N-doped) anodes. For the MEA containing PtRu/C (N-doped), however, the peak changes are more gradual and less severe, suggesting that this cathode is contaminated with smaller amount of Ru species.

Ru contamination in the cathode has been shown to decrease cathode ECSA.<sup>63</sup> The cathode CV measurements as a function of ADT time for both MEAs are provided in Figure 5a-5d. The relative %ECSA loss extracted from H-desorption peaks of the CVs as a function of ADT time is shown in Figure 5e. Both cathodes exhibit well resolved hydrogen adsorption and desorption peaks along with a small double-layer charging current immediately after preconditioning the cell (Fig. 5a). After ADT 200, 400 and 640h (Fig. 5b-5d), the charge associated with the hydrogen adsorption and desorption peaks gradually decreases and the double-layer charging current gradually increases due to the increasing amount of Ru migration from the anode to cathode with increasing ADT duration.<sup>63</sup> The absolute ECSA values for each cathode measured by H-desorption peaks of the CV after different intervals of ADT are given in Table III. ECSA loss is considerably lower for cathode of the MEA containing PtRu/C (N-doped) compared to the cathode of the MEA containing PtRu/C (Hi-SPEC). As can be seen in Fig. 5e, the ECSA loss for cathode of the two MEAs levels off at long ADT durations (400 and 640h). We attribute this effect to the electrochemical formation/conversion and stabilization of Ru higher oxide species that slow down the Ru/RuO<sub>2</sub> and RuO<sub>x</sub>H<sub>y</sub> dissolution from the anodes of PtRu/C (Hi-SPEC) and PtRu/C (N-doped), respectively, at longer ADT durations as previously discussed in Fig. 3.

In order to further probe the influence of migrated Ru on methanol oxidation in the cathode, the methanol crossover current has been measured for both cathodes after 640h ADT (see Figure 6). As shown in this figure, the MOR onset potential occurs at  $\sim 0.3$  and  $\sim 0.27$  V for the cathodes of the MEAs containing PtRu/C (N-doped)

**Table II.** ECSA measured by CO stripping voltammetry for the anode of the MEAs with PtRu/C (N-doped) and PtRu/C (Hi-SPEC).

Catalysts	Before ADT (m <sup>2</sup> g <sup>-1</sup> )	After ADT 80h (m <sup>2</sup> g <sup>-1</sup> )	After ADT 160h (m <sup>2</sup> g <sup>-1</sup> )	After ADT 240h (m <sup>2</sup> g <sup>-1</sup> )	After ADT 280h (m <sup>2</sup> g <sup>-1</sup> )	After ADT 320h (m <sup>2</sup> g <sup>-1</sup> )	After ADT 400h (m <sup>2</sup> g <sup>-1</sup> )	After ADT 560h (m <sup>2</sup> g <sup>-1</sup> )	After ADT 640h (m <sup>2</sup> g <sup>-1</sup> )
PtRu/C (N-doped)	56.1	53.0	51.9	49.30	48.7	43.2	47.0	45.3	44.1
PtRu/C (Hi-SPEC)	126.6	116.0	109.0	105.9	104.2	98.8	98.0	97.0	94.3

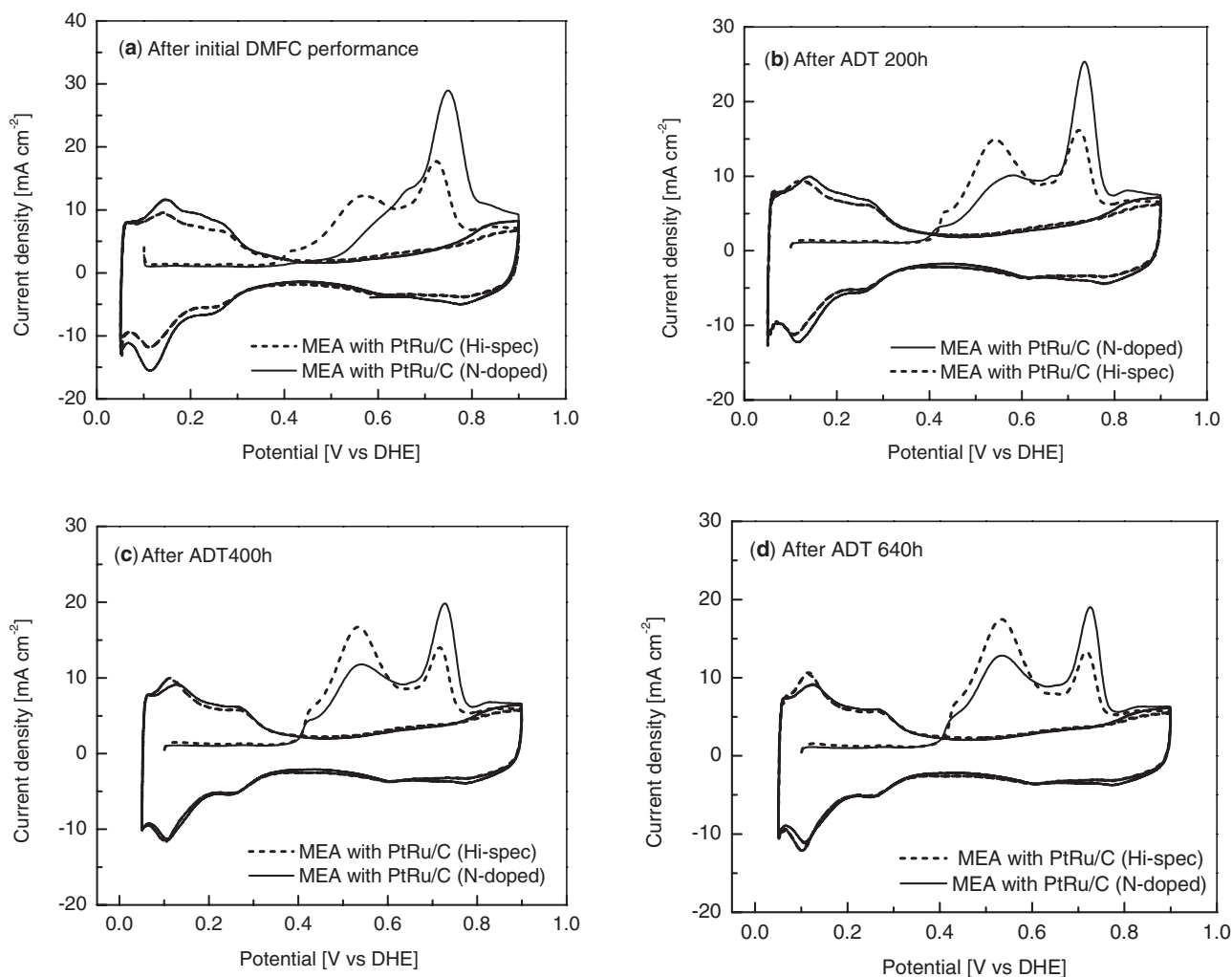


**Figure 4.** Comparison of CO stripping voltammograms for cathodes of the MEAs with PtRu/C (N-doped) and PtRu/C (Hi-SPEC) initially and at various intervals during ADT; (a) After initial DMFC performance (b) After ADT 200h, (c) After ADT 400h and (d) After ADT 640h.

and PtRu/C (Hi-SPEC), respectively. These MOR onset potentials are shifted negatively compared to the MOR onset potential typically associated with pure Pt catalysts ( $\sim 0.4$  V).<sup>64,65</sup> These negative shifts corroborate the presence of Ru in the cathode of the two MEAs. The MEA containing PtRu/C (N-doped) shows a slightly less severe MOR onset potential shift and a 40% lower MOR current density at 0.4 V as compared to the PtRu/C (Hi-SPEC) MEA. This result suggests that the cathode of the MEA containing PtRu/C (N-doped) has a lower amount of Ru contamination after the 640h ADT protocol. The influence of migrated Ru in the cathode on the performance of DMFC requires a detailed investigation. Combined with the previous results from the anode and cathode CO stripping and the cathode CV ECSA measurements, these results reinforce our hypothesis that the nitrogen-modified PtRu/C (N-doped) anode catalyst mitigates  $\text{RuO}_x\text{H}_y$  species loss from PtRu and therefore, the cathode of the MEA containing PtRu/C (N-doped) is significantly less contaminated with Ru after

long-term durability testing. Interestingly, over the duration of the ADT test at 0.8 V, Pt dissolution does not appear to be serious from either anodes, which is evident from increase of Pt at.% against the initial level as will be discussed later in the context of Table V.

*Effect of ADT on DMFC performance.*— A comparison of the DMFC performance for the PtRu/C (N-doped) and PtRu/C (Hi-SPEC) MEAs at various ADT intervals is provided in Figure 7a-7e. Although both MEAs experience rapid initial ECSA loss (due to  $\text{RuO}_x\text{H}_y$ <sup>19,56</sup> and  $\text{Ru/RuO}_2$ <sup>13,57</sup> dissolution from anode of the PtRu/C (N-doped) and PtRu/C (Hi-SPEC), respectively), the open circuit voltage (OCV) and DMFC performances of both MEAs improve significantly during the initial stages of the ADT, as shown in Fig. 7a-7b. The OCV and DMFC performance results at 0.4 V are provided in Table IV. After 200h ADT, both MEAs exhibit identical current

**Table III.** ECSA measured by CV for cathode of the MEAs with PtRu/C (N-doped) and PtRu (Hi-SPEC).

Pt/C Cathode	Before ADT ( $\text{m}^2 \text{g}^{-1}$ )	After ADT 80h ( $\text{m}^2 \text{g}^{-1}$ )	After ADT 160h ( $\text{m}^2 \text{g}^{-1}$ )	After ADT 240h ( $\text{m}^2 \text{g}^{-1}$ )	After ADT 280h ( $\text{m}^2 \text{g}^{-1}$ )	After ADT 320h ( $\text{m}^2 \text{g}^{-1}$ )	After ADT 400h ( $\text{m}^2 \text{g}^{-1}$ )	After ADT 560h ( $\text{m}^2 \text{g}^{-1}$ )	After ADT 640h ( $\text{m}^2 \text{g}^{-1}$ )
MEA with PtRu/C (N-doped)	87.52	78.34	71.34	66.82	64.7	57.0	54.5	53.8	55.5
MEA with PtRu/C (Hi-SPEC)	84.10	70.20	61.25	54.0	53.1	47.45	45.12	45.0	48.5

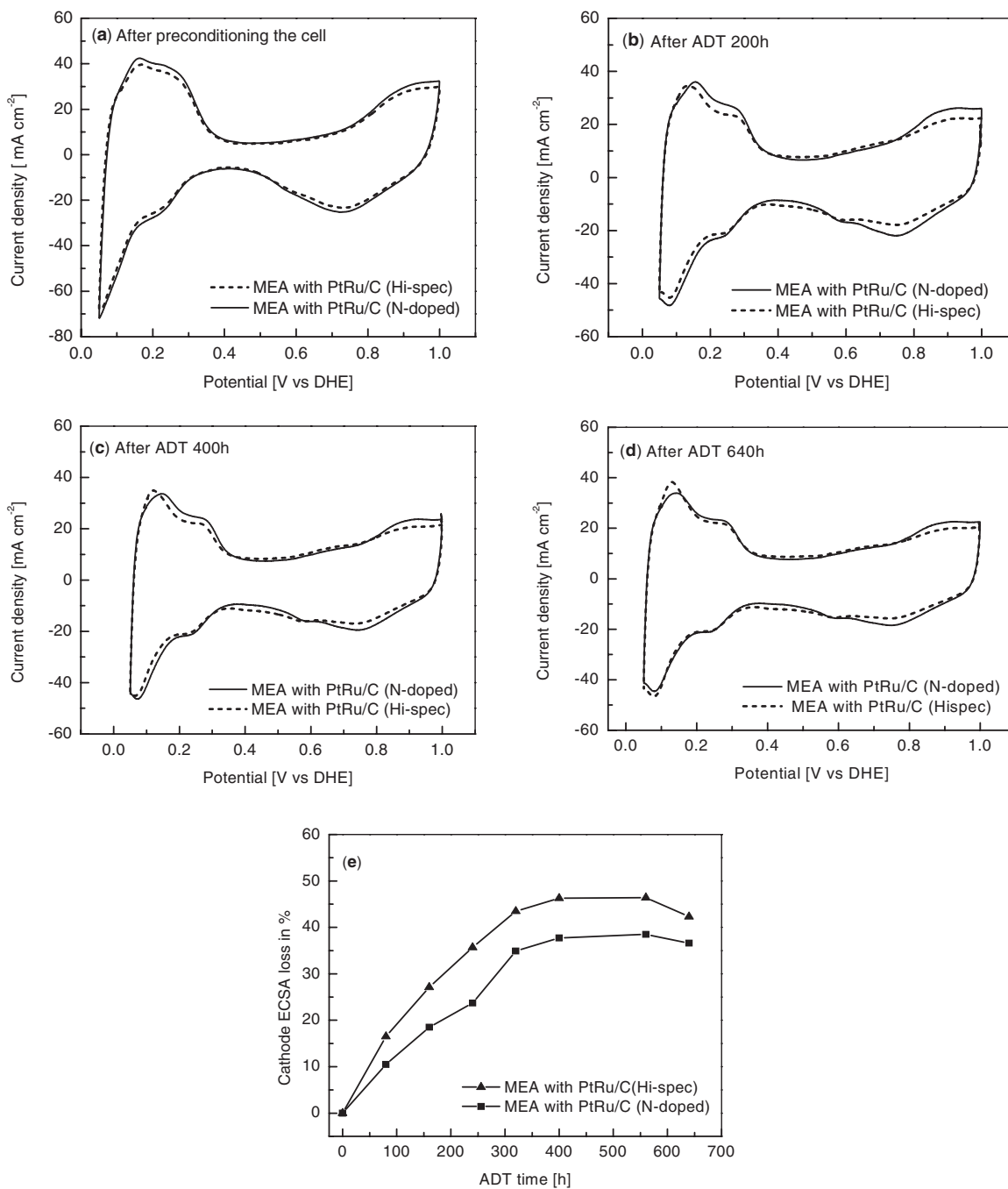


**Figure 5.** Comparison of cathode CVs for the MEAs with PtRu/C (N-doped) and PtRu/C (Hi-SPEC) initially and at various intervals during ADT; (a) After preconditioning the cell, (b) After ADT 200h, (c) After ADT 400h, (d) After ADT 640h and (e) the relative cathode ECSA loss vs. ADT time extracted from H-desorption curves of the CV.

**Table IV.** OCV and DMFC performances of the MEAs with PtRu/C (N-doped) and PtRu/C (Hi-SPEC) tested after different intervals during ADT.

Catalysts	ADT time in h	OCV in volts	Current density mA cm <sup>-2</sup> at 0.4 V	Anode ECSA loss in%
PtRu/C (N-doped)	0	0.720	160	0
	200	0.750	220	9
	400	0.750	170	16
	640	0.745	172	21
PtRu/C(Hi-SPEC)	0	0.745	180	0
	200	0.755	220	15
	400	0.750	175	23
	640	0.750	175	25

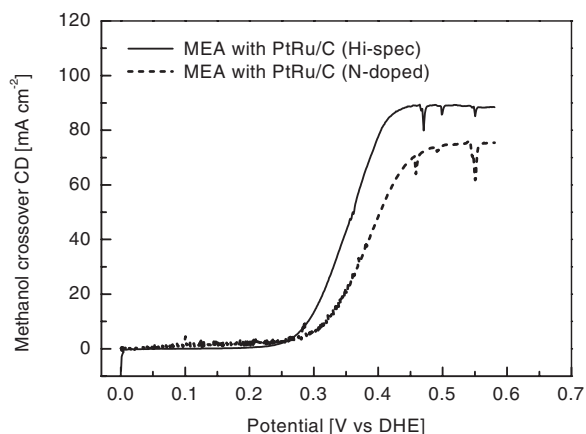


**Figure 6.** Methanol crossover current density (CD) measured at the cathode of the MEAs with PtRu/C (Hi-SPEC) and PtRu/C (N-doped).

densities of  $220 \text{ mA cm}^{-2}$  at  $0.4 \text{ V}$  (Fig. 7c). This amounts to an increase in current density of  $\sim 28$  and  $\sim 20\%$ , respectively, for the PtRu/C (N-doped) and PtRu/C (Hi-SPEC) MEAs despite the fact that the anodes have experienced  $\sim 9$  and  $\sim 15\%$  ECSA loss as shown in Fig. 3c. This observation is contrary to the results reported in the literature, where a severe degradation in a cell performance (using an anode containing PtRu (1:1) black) has been observed after 160h using the same ADT protocol.<sup>8</sup> As previously discussed, the improvement in OCV and cell performance is most likely due to the simultaneous electrochemical formation/conversion of Ru higher oxide species during the ADT at  $0.8 \text{ V}$ , which can be actively involved in the mediation of the MOR during the subsequent DMFC performance testing.<sup>58,59</sup> After 400h ADT, the performances of the MEAs containing PtRu/C (N-doped) and PtRu/C (Hi-SPEC) are observed to be  $170$  and  $175 \text{ mA cm}^{-2}$ , respectively, at  $0.4 \text{ V}$  (Fig. 7d). Almost identical results are observed after 640h ADT (see Table IV and Fig. 7e). As shown in Table IV after long ADTs, current density for the PtRu/C (N-doped) MEA is still  $\sim 8\%$  higher than its initial value, whereas the PtRu/C (Hi-SPEC) MEA has experienced a slight  $\sim 3\%$  decrease in current

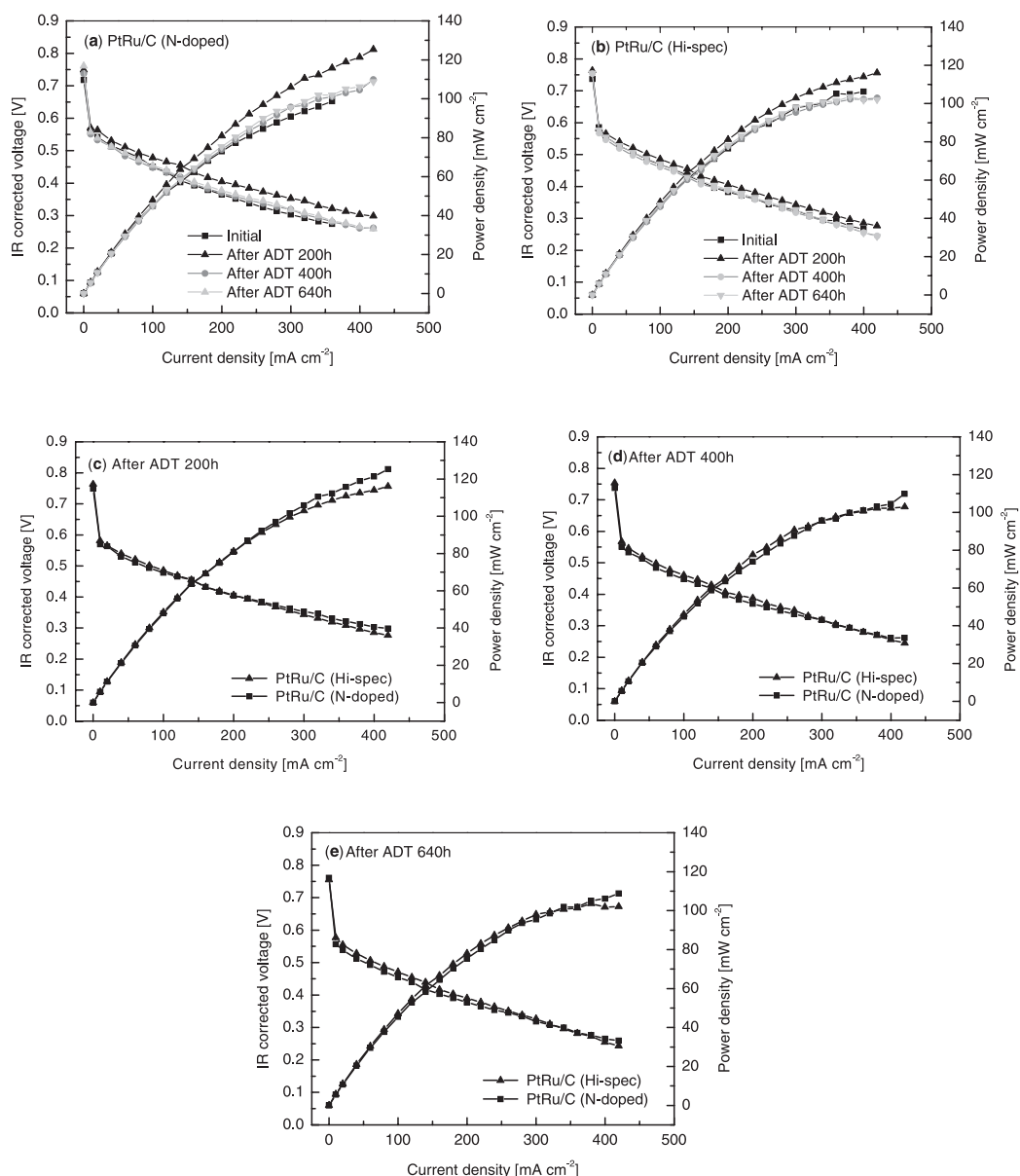


**Figure 7.** Comparison of DMFC performances for the MEAs ( $80^\circ\text{C}$ ) at different intervals during ADT; (a) PtRu/C (N-doped), (b) PtRu/C (Hi-SPEC), (c) after ADT 200h, (d) after ADT 400h and (e) after ADT 640h.

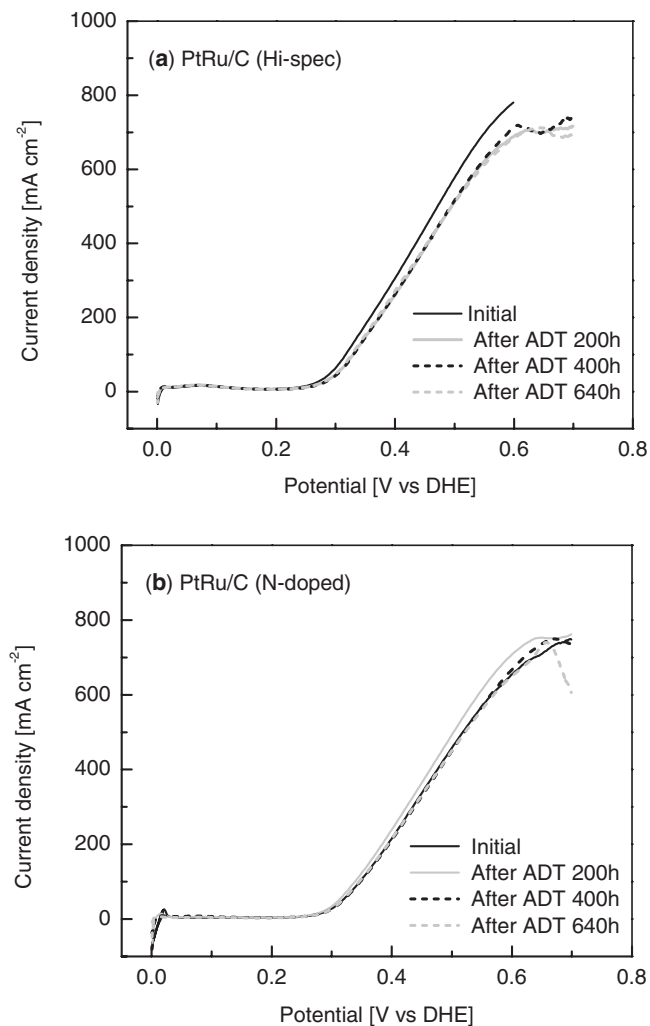
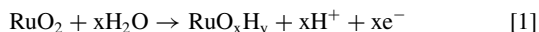


**Figure 8.** MOR activity for anode of the MEAs (80°C) with (a) PtRu/C (Hi-SPEC) and (b) PtRu/C (N-doped) at different intervals during the ADT.

density at 0.4 V. Meanwhile, the corresponding anode ECSA losses for the two MEAs after 640h ADT are  $\sim 20\%$  and  $\sim 26\%$ , respectively.

In order to further probe the phenomenon of improved DMFC performance during ADT, the MOR activity of both anodes were assessed via LSV under the same operating conditions used for DMFC performance testing (1 M methanol, methanol flow rate  $2 \text{ mL min}^{-1}$  and at  $80^\circ\text{C}$ ). The results are shown in Figure 8. For the PtRu/C (Hi-SPEC) anode, the MOR current decreases by  $40 \text{ mA cm}^{-2}$  at 0.4 V after 200h ADT (Fig. 8a). Although this result is contradictory with the observed improvement in the cell performance, it can be attributed to preferred Ru/RuO<sub>2</sub> dissolution taking place from the PtRu/C (Hi-SPEC) anode after the initial stages of ADT. At later intervals of 400 and 640h during ADT, there is no further decrease in the MOR current. This stabilization effect of PtRu/C (Hi-SPEC) anode is most likely due to the simultaneous electrochemical conversion of some of the RuO<sub>2</sub> (see Table I) into RuO<sub>x</sub>H<sub>y</sub> species as shown by the following equation 1 and its involvement in the MOR activity.<sup>58,59</sup>

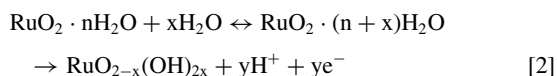


For the PtRu/C (N-doped), on the other hand, the MOR current increases by  $25 \text{ mA cm}^{-2}$  at 0.4 V after 200h ADT (Fig. 8b); this is consistent with significant improvement in the DMFC performance after the initial stages of ADT as shown in Fig. 7a. After 400h ADT, the MOR current decreases by  $25 \text{ mA cm}^{-2}$  and stabilizes thereafter at 0.4 V as seen in Fig. 8b. It is speculated that in the PtRu/C (N-doped), the presence of higher amounts of RuO<sub>x</sub>H<sub>y</sub> or RuO<sub>2</sub> · nH<sub>2</sub>O leads to

**Table V. Atomic% of Pt and Ru in the anode and in the cathode of MEAs subjected to 640h ADT from post-mortem SEM-EDS analysis.**

Anode catalyst in the MEA	Anode composition		Cathode composition	
	Pt, at.%	Ru, at.%	Pt, at.%	Ru, at.%
PtRu/C (Hi-SPEC)	53.9±0.9	46.1±0.9	91.8±0.9	8.2±0.9
PtRu/C (N-doped)	57.7±0.4	42.3±0.4	95.2±1.9	4.8±1.9

greater water absorption on the catalyst surface (the electro-catalytic activity of RuO<sub>2</sub> · nH<sub>2</sub>O depends on amount of water<sup>66</sup>), which can be subsequently converted into surface hydroxides during ADT at 0.8 V as shown in equation 2.<sup>67-70</sup>



The above reaction is likely to take place, besides the dissolution of RuO<sub>x</sub>H<sub>y</sub> species at 0.8 V.<sup>19,56</sup> Our hypothesis is that the nitrogen-doped carbon support has the ability to retain RuO<sub>x</sub>H<sub>y</sub> species in the PtRu catalyst, which in-turn facilitates the electrochemical formation of RuO<sub>2-x</sub>(OH)<sub>2x</sub> species that can actively participate in the MOR after long term ADT. From the DMFC performance and the anode MOR activity data, it is apparent that RuO<sub>x</sub>H<sub>y</sub> species dissolution during the ADT is minimized in the PtRu/C (N-doped) anode while the rapid electrochemical formation of RuO<sub>2-x</sub>(OH)<sub>2x</sub> species appears to be favored, leading to improved long-term performance and greater stability for the N-doped catalyst. The hypothesized adsorption of more amount of water by RuO<sub>x</sub>H<sub>y</sub> and its subsequent conversion into surface hydroxide species (which might have positive influence on the MOR), despite ECSA loss in the anode after being subjected to ADT at high anodic potential requires further investigation in future work.

**SEM-EDS results for MEAs after ADT.**— The MEAs after 640h ADT were dissected in order to probe the atomic compositions of Pt and Ru both in the anode and in the cathode by SEM-EDS. The SEM cross-sectional images and the associated EDS maps for the MEAs containing PtRu/C (Hi-SPEC) and PtRu/C (N-doped) are displayed in Figure 9a-9b, respectively. The Pt and Ru atomic compositions both in the anode and in the cathode are given in Table V. From the Table, it is clear that the at.% Pt in both anode catalysts increases as compared to their initial level (see Table I). The PtRu/C (Hi-SPEC) has initial Pt content of 50 at.% and after 640h ADT it shows a value close to 54 at.%. The PtRu/C (N-doped) catalyst has an initial Pt content of 52.6 at.% and after 640h ADT it increases to 57.7 at.%. The enrichment in Pt can be related with loss of Ru from the anode of both the catalysts. These results confirm that Ru dissolution rather than Pt dissolution is predominant from the anodes of both MEAs during the ADT test at 0.8 V.

In the cathode side of both MEAs, the presence of Ru species after ADT is prominent from the SEM/EDS cross-section images. Detailed EDS mapping has been carried out to quantify the Ru content at various distances from the membrane/cathode interface for both MEAs (Figure 10a-10b). The at.% Ru values for each MEA as a function of distance from the membrane/cathode interface are depicted in Fig. 10c. In both the MEAs, the Ru content is highest near the membrane/cathode interface and gradually decreases further out into the bulk of the catalyst layer. However, significantly less Ru is found in the cathode of the MEA containing the PtRu/C (N-doped) anode ( $\sim 4.8$  at.% cathode-averaged Ru content) vs. the MEA containing the PtRu/C (Hi-SPEC) anode ( $\sim 8.2$  at.% cathode-averaged Ru content). This observation is in good correlation with our CO stripping, CV and methanol crossover current results and discussions and substantiates the preventative effect of the N-doped carbon anode on mitigating Ru/RuO<sub>x</sub>H<sub>y</sub> dissolution and cross-over problems.

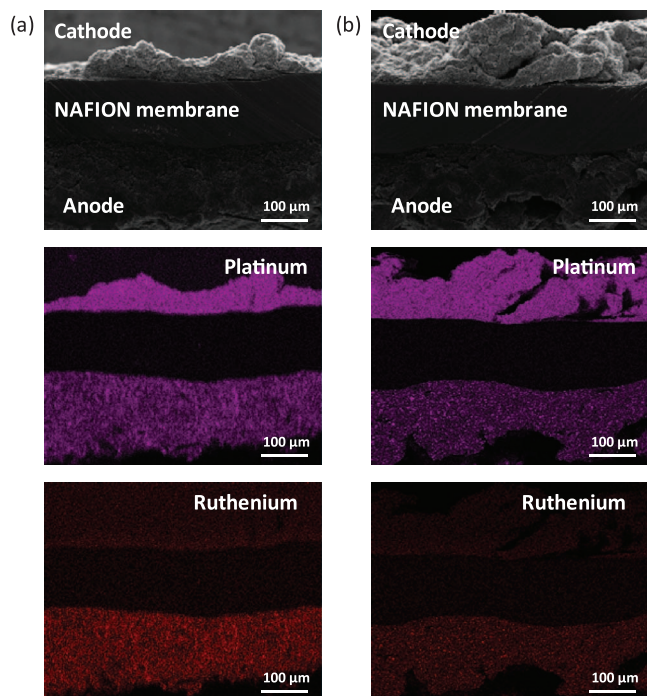


**Figure 9.** SEM-EDS mapping for anode and cathode of the dissected MEAs after 640h ADT; (a) PtRu/C (Hi-SPEC) and (b) PtRu/C (N-doped).

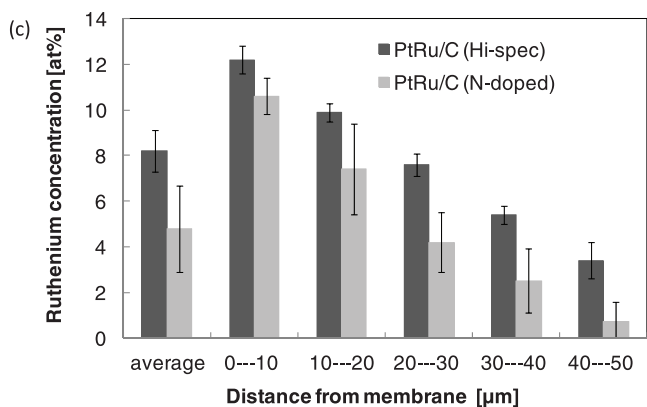
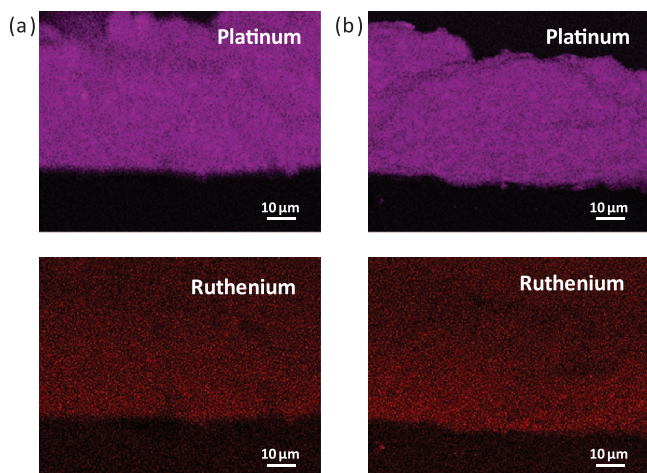


**Figure 10.** SEM-EDS mapping showed the existence of Ru at the cathode interface of the dissected MEAs after 640h ADT (a) PtRu/C (Hi-SPEC), (b) PtRu/C (N-doped) and (c) the at.% Ru values measured in the cathode catalyst layer at various distances from the membrane/cathode interface.

## Conclusions

The MEA based on the PtRu/C (N-doped) anode exhibited slightly lower initial DMFC performance compared to the MEA based on the commercial PtRu/C (Hi-SPEC) anode because of the significantly lower ECSA of the former catalyst. However, the performance of the two MEAs equalized after different stages of ADT and the relative anode ECSA loss incurred by the MEA containing the PtRu/C (N-doped) anode was found to be  $\sim 5\%$  less than for the PtRu/C (Hi-SPEC) anode. This effect is attributed to a significant mitigation in  $\text{RuO}_x\text{H}_y$  dissolution for the PtRu/C (N-doped) anode during the ADT. Furthermore, CO stripping, cathode CV, and methanol crossover current studies substantiated that the cathode of the PtRu/C (N-doped) MEA experienced significantly less Ru contamination than the cathode of the PtRu/C (Hi-SPEC) MEA. As a result, the relative cathode ECSA loss incurred by the PtRu/C (N-doped) MEA was found to be  $\sim 7\%$  less than for the PtRu/C (Hi-SPEC) MEA after 640h ADT. The post-mortem SEM-EDS results of both MEAs after 640h ADT indicated a significantly larger amount of Ru contamination in the cathode of the PtRu/C (Hi-SPEC) MEA compared to the cathode of the PtRu/C (N-doped) MEA ( $\sim 8.2$  Ru at.% vs.  $\sim 4.8$  Ru at.%). For both MEAs, the DMFC performance improved, especially after the initial stages of ADT, despite the anode and cathode ECSA losses. Interestingly, the MEA based on the PtRu/C (N-doped) anode shows performance improvements of  $\sim 28$  and  $\sim 8\%$  after initial (200h) and long-term (400 and 640h) ADT, respectively. In contrast, the MEA based on the commercial PtRu/C (Hi-SPEC) anode shows a performance improvement of  $\sim 20\%$  after 200h ADT and an overall performance decrease of  $\sim 3\%$  after long-term (400 and 640h) ADT. It is concluded that the significant improvements in the DMFC performance and the mitigation of  $\text{RuO}_x\text{H}_y$  species dissolution observed for the MEA with PtRu/C (N-doped) is mainly attributed to the ability of the nitrogen-doped carbon support to enhance the retention of  $\text{RuO}_x\text{H}_y$  in the anode during ADT at 0.8 V.

## Acknowledgments

This work is supported by the Army Research Office under grant #W911NF-09-1-0528 at CSM. The work at NREL is supported by the U.S. Department of Energy EERE, FCT Program, under Contract No. DE-AC36-08-GO28308 with the National Renewable Energy Laboratory. The authors also acknowledge Electron Microscopy Laboratory at CSM.

## References

1. B. McNicol, D. Rand, and K. Williams, *J. Power Source*, **83**, 5 (1999).
2. K. B. Prater, *J. Power Sources*, **61**, 9 (1996).
3. A. S. Arico, S. Srinivasan, and V. Antonucci, *Fuel Cells*, **1**, 61 (2001).
4. J. T. Wang, S. Wasmus, and R. F. Savinell, *J. Electrochem. Soc.*, **143**, 1233 (1996).
5. P. Pielak, C. Eickes, E. Brosha, F. Garzon, and F. Zeleny, *J. Electrochem. Soc.*, **153**, A171 (2006).
6. S. D. Knights, K. M. Colbow, J. St-Pierre, and D. P. Wilkinson, *J. Power Sources*, **127**, 127 (2004).
7. Z.-B. Wang, X.-P. Wang, P.-J. Zuo, B.-Q. Yang, G.-P. Yin, and X.-P. Feng, *J. Power Sources*, **181**, 93 (2008).
8. C.-M. Lai, J.-C. Lin, K.-L. Hsueh, C.-P. Hwang, K.-C. Tsay, L.-D. Tsai, and Y.-M. Peng, *J. Electrochem. Soc.*, **155**(8), B843 (2008).
9. J.-Y. Park, M. A. Scibioh, S.-K. Kim, H.-J. Kim, I.-H. Oh, T. G. Lee, and H. Y. Ha, *Int J. Hydrogen Energy*, **34**, 2043 (2009).
10. J. Prabhuram, N. N. Krishnan, B. Choi, T.-H. Lim, H. Y. Ha, and S.-K. Kim, *Int. J. Hydrogen Energy*, **35**, 6924 (2010).
11. M. K. Jeon, K. R. Lee, K. S. Oh, D. S. Hong, J. Y. Won, S. Li, and S. I. Woo, *J. Power Sources*, **158**, 1344 (2006).
12. A. K. Shukla, C. L. Jackson, K. Scott, and R. K. Raman, *Electrochim. Acta.*, **47**, 3401 (2002).
13. P. Pielak, C. Eickes, E. Brosha, F. Garzon, and P. Zelenay, *J. Electrochem. Soc.*, **151**(2), A2053 (2004).
14. J. Liu, Z. Zhou, X. Zhao, Q. Xin, G. Sun, and B. Yi, *Phys. Chem. Chem. Phys.*, **6**, 134 (2004).
15. H. Kim, S.-J. Shin, Y. Park, J. Song, and H. Kim, *J. Power Sources*, **160**, 440 (2006).
16. L. Li, J. Zhang, and Y. Wang, *J. Membr. Sci.*, **226**, 159 (2003).
17. Y. S. Kim, W. L. Harrison, J. E. McGrath, and B. S. Pivovar, *205<sup>th</sup> ECS meeting*, Abs. **334**, (2004).
18. E. Antolini, *J. Solid State Electrochem.*, **15**, 455 (2011).

19. K.-H. Chang and C.-C. Hu, *J. Electrochem. Soc.*, **151**, A958 (2004).
20. W. Sugimoto, T. Saida, and Y. Takasu, *Electrochem. Comm.*, **8**, 411 (2006).
21. T. Saida, W. Sugimoto, and Y. Takasu, *Electrochim. Acta*, **55**, 857 (2010).
22. Z. X. Liang, T. S. Zhao, and J. B. Xu, *J. Power Sources*, **185**, 185 (2008).
23. S. Garbarino, A. Ponrouch, S. Pronovost, and D. Guay, *Electrochem. Commun.*, **11**, 1449 (2009).
24. A. S. Aarnio, M. Borghei, I. Anoshkin, A. G. Nasbulin, E. I. Kauppinen, V. Ruiz, and T. Kallio, *Int. J. Hydrogen Energy*, **37**, 3415 (2012).
25. S. Kang, S. Lim, D.-H. Peck, S.-K. Kim, D.-H. Jung, S.-H. Hong, H.-G. Jung, and Y. Shul, *Int. J. Hydrogen Energy*, **37**, 4685 (2012).
26. C.-H. Wang, H.-C. Shih, Y.-T. Tsai, H.-Y. Du, L.-C. Chen, and K.-H. Chen, *Electrochim. Acta*, **52**, 1612 (2006).
27. G. Wu, R. Swaidan, D. Li, and N. Li, *Electrochim. Acta*, **53**, 7266 (2008).
28. R. Chetty, S. Kundu, W. Xia, M. Bron, W. Schuhmann, V. Chirila, W. Brandl, T. Reineke, and M. Muhler, *Electrochim. Acta*, **54**, 4208 (2009).
29. Y. Zhou, R. Pasquarelli, T. Holme, J. Berry, D. Ginley, and R. O'Hayre, *J. Materials Chem.*, **19**, 7830 (2009).
30. Y. Zhou, K. Neyerlin, T. S. Olson, S. Pylypenko, J. Bult, H. N. Dinh, T. Gennett, Z. Shao, and R. O'Hayre, *Energy & Environmental Sci.*, **3**, 1437 (2010).
31. F. Su, Z. Tian, C. K. Poh, Z. Wang, S. H. Lim, Z. Liu, and J. Lin, *Chem. Mater.*, **22**, 832 (2010).
32. S. Pylypenko, A. Queen, T. S. Olson, A. Dameron, K. O' Neill, K. C. Neyerlin, B. Pivovar, H. N. Dinh, D. S. Ginley, T. Gennett, and R. O'Hayre, *J. Phys. Chem. C*, **115**, 13667 (2011).
33. R. Lv, T. Cui, M.-S. Jun, Q. Zhang, A. Cao, D. S. Su, Z. Zhang, S.-H. Yoon, J. Miyawaki, I. Mochida, and F. Kang, *Adv. Funct. Mater.*, **21**, 999 (2011).
34. C.-H. Hsu and P.-L. Kuo, *J. Power Sources*, **198**, 83 (2012).
35. S. Wang, X. Wang, and S. P. Jiang, *Langmuir*, **24**, 10505 (2008).
36. J. Prabhuram, T. S. Zhao, Z. K. Tang, R. Chen, and Z. X. Liang, *J. Phys. Chem. B*, **110**, 5245 (2006).
37. J. Prabhuram, T. S. Zhao, Z. K. Tang, and R. Chen, *Electrochim. Acta*, **52**, 2649 (2007).
38. S.-H. Liu, M.-T. Wu, Y.-H. Lai, C.-C. Chiang, N. Yu, and S.-B. Liu, *J. Mater. Chem.*, **21**, 12489 (2011).
39. B. Choi, H. Yoon, I.-S. Park, J. Jang, and Y.-E. Sung, *Carbon*, **45**, 2496 (2007).
40. B. Yu, Y. W. Ma, H. S. Tao, L. S. Yu, G. Q. Jian, X. Z. Wang, X. S. Wang, Y. N. Lu, and Z. Hu, *J. Mater. Chem.*, **18**(15), 1747 (2008).
41. R. I. Jafri, N. Rajalakshmi, and S. Ramaprabhu, *J. Power Sources*, **195**(24), 8080 (2010).
42. R. I. Jafri, N. Rajalakshmi, and S. Ramaprabhu, *J. Mater. Chem.*, **20**(34), 7114 (2010).
43. Y. Y. Shao, J. H. Sui, G. P. Yin, and Y. Z. Gao, *Appl. Catal B-Envn.*, **79**(1-2), 89 (2008).
44. M. N. Groves, A. S. W. Chan, C. M. Jugroot, and M. Jugroot, *Chemical Physics Lett.*, **481**(4-6), 214 (2009).
45. C. K. Acharya, D. I. Sullivan, and C. H. Turner, *J. Phys. Chem. C*, **112**(35), 13067 (2008).
46. S. Pylypenko, A. Queen, T. S. Olson, A. Dameron, K. O' Neill, K. C. Neyerlin, B. Pivovar, H. N. Dinh, D. S. Ginley, T. Gennett, and R. O'Hayre, *J. Phys. Chem. C*, **115**(28), 13676 (2011).
47. C.-M. Lai, J.-C. Lin, K.-L. Hsueh, C.-P. Hwang, K.-C. Tsay, L.-D. Tsai, and Y.-M. Peng, *J. Electrochem. Soc.*, **155**(8), B843 (2008).
48. A. R. Corpuz, T. S. Olson, P. Joghee, S. Pylypenko, A. A. Dameron, H. N. Dinh, K. J. O'Neill, K. E. Hurst, G. Bender, T. Gennett, B. S. Pivovar, R. M. Richards, and R. P. O'Hayre, *J. Power Sources*, **217**, 142 (2012).
49. A. Dameron, T. S. Olson, S. T. Christensen, J. E. Leisch, K. E. Hurst, S. Pylypenko, J. B. Bult, D. S. Ginley, R. P. O'Hayre, H. N. Dinh, and T. Gennett, *ACS. Catalysis*, **1**(10), 1307 (2011).
50. C. Mun, J. J. Ehrhardt, J. Lambert, and C. Madic, *Appl. Surface Sci.*, **253**, 7613 (2007).
51. J. H. Cho, J. M. Kim, J. Prabhuram, S. Y. Hwang, D. J. Ahn, and H. Y. Ha, *J. Power Sources*, **187**, 187 (2009).
52. M. Inoue, T. Iwasaki, K. Sayama, and M. Umeda, *J. Power Sources*, **195**, 5986 (2010).
53. X. Ren and S. Gottesfeld, *J. Electrochem. Soc.*, **147**(2), 466 (2000).
54. G. Vijayaragavan and K. J. Stevenson, *Langmuir*, **23**(10), 5279 (2007).
55. D. C. Higgins, D. Meza, and Z. W. Chen, *J. Phys. Chem. C*, **114**(50), 21988 (2010).
56. J. Ma, J. Hu, D. Zhao, A. J. Wang, and B. Q. Xu, *Chinese J. Catal.*, **30**, 485 (2009).
57. Y. Park, B. Lee, C. Kim, Y. Oh, S. Nam, and B. Park, *J. Mater. Res.*, **24**, 2762 (2009).
58. Q. Lu, B. Yang, L. Zhuang, and J. Lu, *J. Phys. Chem. B*, **109**, 1715 (2005).
59. M. K. Jeon, J. Y. Won, and S. I. Woo, *Electrochem. Solid-state Lett.*, **10**(1), B23 (2007).
60. K. N. Wood, S. T. Christensen, S. Pylypenko, T. S. Olson, A. Dameron, K. E. Hurst, H. N. Dinh, T. Gennett, and R. O'Hayre, *MRS Communications*, Available on CJO July 2012.
61. J.-H. Choi, Y. S. Kim, R. Bashyam, and P. Zelenay, *ECS Trans.*, **1**(8), 437 (2006).
62. H. A. Gasteiger, N. Markovic, P. N. Ross Jr., and E. J. Cairns, *J. Phys. Chem.*, **98**, 617 (1994).
63. L. Gancs, B. N. Hult, N. Hakim, and S. Mukerjee, *Electrochem. Solid-state Lett.*, **10**(9), B150 (2007).
64. C.-L. Sun, L.-C. Chen, M.-C. Su, L.-S. Hong, O. Chyan, C.-Y. Hsu, K.-H. Chen, T.-F. Chang, and L. Chang, *Chem. Mater.*, **17**, 3749 (2005).
65. F. Su, Z. Tian, C. K. Poh, Z. Wang, S. H. Lim., Z. Liu, and J. Lin, *Chem. Mater.*, **22**, 832 (2010).
66. W. Dmowski, T. Egami, K. E. S. Lyons, C. T. Love, and D. R. Rolison, *J. Phys. Chem. B*, **106**, 12677 (2002).
67. W. L. Holstein and H. D. Rosenfeld, *J. Phys. Chem. B*, **109**, 2176 (2005).
68. D. R. Rolison, P. L. Hagans, K. E. Swider, and J. W. Long, *Langmuir*, **15**, 774 (1999).
69. H. M. Villullas, F. I. Mattos-Costa, and L. O. S. Bulhoes, *J. Phys. Chem., B*, **108**, 12898 (2004).
70. S.-Y. Huang, C.-M. Chang, K.-W. Wang, and C.-T. Yeh, *Chem. Phys. Chem.*, **8**, 1774 (2007).